

NJC

Accepted Manuscript



This is an *Accepted Manuscript*, which has been through the Royal Society of Chemistry peer review process and has been accepted for publication.

Accepted Manuscripts are published online shortly after acceptance, before technical editing, formatting and proof reading. Using this free service, authors can make their results available to the community, in citable form, before we publish the edited article. We will replace this *Accepted Manuscript* with the edited and formatted *Advance Article* as soon as it is available.

You can find more information about *Accepted Manuscripts* in the [Information for Authors](#).

Please note that technical editing may introduce minor changes to the text and/or graphics, which may alter content. The journal's standard [Terms & Conditions](#) and the [Ethical guidelines](#) still apply. In no event shall the Royal Society of Chemistry be held responsible for any errors or omissions in this *Accepted Manuscript* or any consequences arising from the use of any information it contains.

ARTICLE

Hydrogen photogeneration catalyzed by a cobalt complex of pentadentate aminopyridine-based ligand

Cite this: DOI: 10.1039/x0xx00000x

Xiaowei Song^{a,b}, Huimin Wen^a, Chengbing Ma^a, Hui Chen^a and Changneng Chen^{a*}

Received 00th January 2012,

Accepted 00th January 2012

DOI: 10.1039/x0xx00000x

www.rsc.org/

A pentadentate aminopyridine ligand [(9-methyl-1,10-phenanthrolin-2-yl)methyl]bis(pyridin-2-ylmethyl)amine (DPA-Dmphen) has been prepared and characterized. This ligand readily accommodates Co(II) or Ni(II) bearing a coordinated apical water ligand, and the resulting complexes of general formula $[M(\text{Dmphen-DPA})(\text{H}_2\text{O})](\text{ClO}_4)_2$ ($M=\text{Co}$ (**1**) and $M=\text{Ni}$ (**2**)) have been investigated for photo- and electrocatalytic proton reduction in $\text{CH}_3\text{CN-H}_2\text{O}$ (1/3, v/v) mixed solvent and CH_3CN , respectively. Under visible-light irradiation ($\lambda > 400$ nm), the complex **1** shows hydrogen evolution activity when in presence of $[\text{Ir}(\text{ppy})_2(\text{bpy})]\text{PF}_6$ as photosensitizer and TEA as electron donor, whereas **2** displays much lower catalytic activity under the same conditions. Highest turnover numbers (TONs) of 210 for H_2 evolution are achieved from an optimized system containing **1** (0.1 mM), $[\text{Ir}(\text{ppy})_2(\text{bpy})](\text{PF}_6)$ (0.5 mM), and 10 vol% TEA in $\text{CH}_3\text{CN-H}_2\text{O}$ (1/3, v/v) mixed solvents at pH 10. Under those conditions catalytic hydrogen production is mainly limited by photosensitizer and catalyst stability. Furthermore, electrochemical studies reveal that both complexes are active for electrocatalytic proton reduction in acetonitrile, when using acetic acid as a proton source with overpotentials for **1** (0.48 V vs. Fc^+/Fc) and **2** (0.46 V vs. Fc^+/Fc).

1. Introduction

Energy-rich and “green” hydrogen has attracted considerable attention because it holds great promise for addressing the ever-increasing demand for energy and climate change of today’s society.¹ Among the currently available options for obtaining hydrogen, visible-light-driven hydrogen evolution from water is an ecofriendly and fascinating way.² Therefore, a number of highly efficient hydrogen evolving systems have been described including homogeneous and heterogeneous photocatalytic systems.³ Studies on the homogeneous catalysts for hydrogen production are mainly focused on the earth abundant molecular complexes based on iron,⁴ cobalt,⁵ nickel,⁶ and molybdenum.⁷ Among these catalysts, cobalt- and nickel-based catalysts are pretty good at catalyzing the reduction of protons to hydrogen under mild conditions.⁸ In particular, since the cobalt bipyridine complex $[\text{Co}(\text{bpy})_3]^{2+}$ was found as an efficient H_2 -evolving precatalyst,⁹ an increasing number of cobalt complexes of polypyridyl platform have been developed as catalysts for photoinduced hydrogen evolution.^{8b, 10}

Recently, many cobalt complexes based on versatile aminopyridine ligands (Fig. 1) have served as electro- and

photocatalysts for hydrogen generation. For instance, Zhao and Webster *et al.* reported a very active cobalt complex supported by a pentadentate aminopyridine ligand (DPA-Bpy), which displayed remarkable efficiencies towards photocatalytic hydrogen production in combination with $[\text{Ru}(\text{bpy})_3]^{2+}$ as photosensitizer and ascorbic acid as electron donor, with turnover numbers (TONs) of up to 4400.^{10c, 11} A similar cobalt complex ligated by a tripyridine-diamine pentadentate ligand (bztpen) was demonstrated to facilitate the generation of hydrogen from purely aqueous solution.¹² Not long ago, Lloret-Fillol also described a cobalt complex with an aminopyridine pentadentate ligand ($\text{Py}_2^{\text{Tstacn}}$), which functioned as an efficient catalyst for proton reduction to hydrogen. This complex, associated with $[\text{Ir}(\text{ppy})_2(\text{bpy})]\text{PF}_6$ as photosensitizer and triethylamine (TEA) as electron donor, could reach 660 TONs after 1.5 h of photocatalysis reaction.¹³

Cobalt aminopyridine complexes have drawn great attention due to their impressive stability and excellent catalytic activity for hydrogen generation. To extend the aminopyridine ligand, we synthesized a pentadentate aminopyridine ligand [(9-methyl-1,10-phenanthrolin-2-yl)methyl]bis(pyridin-2-ylmethyl)amine (DPA-Dmphen), as well as its corresponding cobalt and nickel complexes. The resultant cobalt complex **1**

presents significant proton reduction activity in electro- and photocatalytic experiments, while the nickel complex **2** only displays electrocatalytic activity. Drawings of the complexes are presented in Fig. 1.

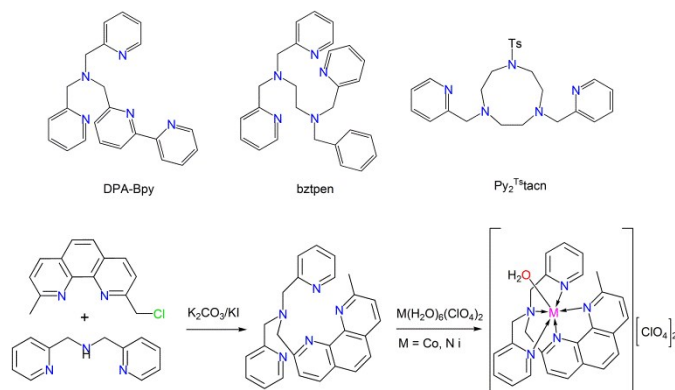


Fig. 1 Aminopyridine-containing ligands reported in the literature and synthetic procedure for the complexes in the present work.

2. Experimental section

2.1. General procedures and chemicals

All reactions were carried out under a dry nitrogen atmosphere by using Schlenk techniques and vacuum-line systems unless otherwise specified. The solvents were dried, distilled, and degassed prior to use except that those for spectroscopic measurements were of spectroscopic grade. The syntheses of $[\text{Ir}(\text{ppy})_2(\text{bpy})](\text{PF}_6)$,¹⁴ 2-(chloromethyl)-9-methyl-1,10-phenanthroline¹⁵ and bis(pyridin-2-ylmethyl)amine¹⁶ were performed according to literature procedures. Other chemicals in this work were purchased from commercial sources and used without further purification. Elemental analyses were carried out on a Vario MICRO Elemental Analyser. ^1H , ^{13}C NMR spectra were performed on a Bruker Avance III (400 MHz) spectrometer. Electrospray ionization mass spectra (ESI-MS) were recorded on a Finnigan DECA-X-30000 LCQ mass spectrometer. Emission spectra in degassed solutions were recorded on a Perkin-Elmer LS55 luminescence spectrometer.

2.2. Synthesis

[(9-methyl-1,10-phenanthrolin-2-yl)methyl]bis(pyridin-2-ylmethyl)amine (Dmphen-DPA). A stirred mixture of 2-(chloromethyl)-9-methyl-1,10-phenanthroline (0.48 g, 2 mmol), bis(pyridin-2-ylmethyl)amine (0.40 g, 2 mmol), potassium carbonate (0.55 g, 4 mmol) and potassium iodide (0.32 g, 2 mmol) in acetonitrile (50 mL) was heated at 80 °C under a N_2 atmosphere for 24 h. After the reaction solvent was evaporated, water (50 mL) was added. The product was extracted into dichloromethane (3×20 mL). The combined organic layers were dried over anhydrous Na_2SO_4 , filtered, and evaporated under reduced pressure to afford the crude compound. The crude product was purified by column chromatography (silica gel) with CH_2Cl_2 - CH_3OH -ammonia (5:1:0.2, v/v/v) as eluent to give pure ligand. ^1H NMR (400 MHz, CDCl_3) 8.58 (2 H, d, $J=4.4$),

8.26 (1 H, d, $J=8.3$), 8.15 (2 H, dd, $J=8.2, 3.3$), 7.81-7.62 (6 H, m), 7.51 (1 H, d, $J=8.2$), 7.23-7.11 (2 H, m), 4.36 (2 H, s), 4.01 (4 H, s), 2.96 (3 H, s). ^{13}C NMR (101 MHz, CDCl_3) 159.45, 159.19, 149.20, 145.38, 145.28, 136.76, 136.53, 136.28, 127.73, 126.83, 125.94, 125.44, 123.60, 123.17, 122.09, 121.80, 60.75, 60.34, 25.98. ESI-MS: calculated for $[\text{M}+\text{H}]^+$ ($\text{C}_{26}\text{H}_{24}\text{N}_5$): m/z 406.20; found: 406.1.

Preparation for the compound $[\text{Co}(\text{Dmphen-DPA})(\text{H}_2\text{O})](\text{ClO}_4)_2$ (1**)** Under a nitrogen atmosphere, CH_3OH (15 mL) was added to an equimolar mixture of metal salt $\text{Co}(\text{H}_2\text{O})_6(\text{ClO}_4)_2$ (0.18 g, 0.49 mmol) and ligand Dmphen-DPA (0.21 g, 0.5 mmol); and the resulting solution was stirred at room temperature. After 10 h, the solid materials of the desired metal complexes were precipitated by addition of diethyl ether (20 mL) to the reaction solution. The powders were collected by filtration, washed with diethyl ether (3×5 mL), and recrystallized by diethyl ether diffusion to yield the crystalline material of red **1** (0.26 g, 76%). Anal. Calcd for $\text{C}_{26}\text{H}_{25}\text{Cl}_2\text{CoN}_5\text{O}_9 \cdot 2\text{H}_2\text{O}$: C, 43.53%; H, 4.07%; N, 9.76%. Found: C, 43.46%; H, 4.35%; N, 9.54%. ESI-MS: calculated for $[\text{M}-\text{ClO}_4-\text{H}_2\text{O}]^+$ ($\text{C}_{26}\text{H}_{23}\text{ClCoN}_5\text{O}_4$): m/z 563.08; found: 563.1.

Preparation for the compound $[\text{Ni}(\text{Dmphen-DPA})(\text{H}_2\text{O})](\text{ClO}_4)_2$ (2**)** **2** was prepared in an analogous manner to **1** using $\text{Ni}(\text{H}_2\text{O})_6(\text{ClO}_4)_2$ (0.18 g, 0.49 mmol) to give 0.29 g (88%) of product as pale brown crystals. Anal. Calcd for $\text{C}_{26}\text{H}_{25}\text{Cl}_2\text{NiN}_5\text{O}_9$: C, 45.83%; H, 3.70%; N, 10.28%. Found: C, 45.57%; H, 3.60%; N, 10.02%. ESI-MS: calculated for $[\text{M}-\text{ClO}_4-\text{H}_2\text{O}]^+$ ($\text{C}_{26}\text{H}_{23}\text{ClNiN}_5\text{O}_4$): m/z 562.08; found: 562.1.

2.3. Crystal structure determination

Single crystals of **1** and **2**, suitable for X-ray diffraction analysis, were grown by slow diffusion of diethyl ether into the methanol solution of the complexes. The X-ray single crystal data were collected on the Agilent Supernova Dual (Cu at zero) Atlas diffractometer. Crystal data collection, refinement and reduction were accomplished with the CrysAlisPro, Agilent Technologies, and Version 1.171.37.33. The crystal structures were solved by direct methods with SHELXS-97 and refined by using the SHELXL-97 crystallographic software package. All non-hydrogen atoms were refined anisotropically. The hydrogen atoms were added in a riding model. Details of crystal data are summarized in Table 1. CCDC-1028564 and CCDC-1028563 (for **1** and **2**) contain the supplementary crystallographic data for this paper.

2.4. Photocatalysis

In a typical procedure, $[\text{Ir}(\text{ppy})_2(\text{bpy})]\text{PF}_6$ (2.0 mg, 2.5 μmol), **1** (0.3 mg, 0.5 μmol) and 5 mL acetonitrile aqueous solution (1/3, v/v) containing 10 vol% TEA were added to a Schlenck bottle. The mixture was magnetically stirred under nitrogen atmosphere for 15 min. The system was freeze-pump-thaw degassed for three times and then warmed to room temperature prior to irradiation. The reaction solution was irradiated at 25 °C using a Xe lamp (300 W) with a cutoff filter ($\lambda > 400$ nm). The gas phase of the reaction system was analyzed on a

GC 7900 instrument with a 5 Å molecular sieve column, a thermal conductivity detector, and using nitrogen as carrying gas. The amount of hydrogen generated was determined by the external standard method. Hydrogen dissolved in the solution was not measured and the slight effect of the hydrogen generated on the pressure of the Schlenk bottle was neglected for calculation of the volume of hydrogen gas.

Table 1 Crystal data and structure refinement details for complexes **1** and **2**

Complex	1	2
Molecule formula	C ₂₆ H ₂₅ Cl ₂ CoN ₅ O ₉	C ₂₆ H ₂₅ Cl ₂ N ₅ NiO ₉
Formula weight	681.34	681.12
<i>T</i> (K)	100.0(2)	99.99(17)
Crystal system	Monoclinic	Monoclinic
Space group	<i>P</i> 2 ₁ / <i>c</i>	<i>P</i> 2 ₁ / <i>c</i>
<i>a</i> (Å)	15.5452(2)	15.5059(3)
<i>b</i> (Å)	11.45475(14)	11.4074(2)
<i>c</i> (Å)	16.1105(2)	16.1421(3)
α (°)	90	90
β (°)	99.8494(12)	100.0360(16)
γ (°)	90	90
<i>V</i> (Å ³)	2826.45(6)	2811.56(9)
<i>Z</i>	4	4
<i>F</i> (000)	1396	1400
<i>D</i> _{calc} (g cm ⁻³)	1.601	1.609
<i>R</i> ₁ / <i>wR</i> ₂ (<i>I</i> > 2σ(<i>I</i>))	0.0308/0.0751	0.0421/0.1041
<i>R</i> ₁ / <i>wR</i> ₂ (all data)	0.0371/0.0781	0.0510/0.1093
Goodness-of-fit	1.035	1.054

2.5. Electrochemistry

Electrochemical measurements were made using a CH instrument Model 630A electrochemical workstation. The cyclic voltammetry experiments were conducted on in a three electrode cell including a glassy carbon working electrode, a Pt wire auxiliary electrode, and a Ag/AgCl reference electrode under nitrogen atmosphere. The potential was reported relative to the internal reference of Fc⁺/Fc = 0.00 V. The supporting electrolyte was 0.1 M Bu₄NPF₆ in acetonitrile.

3. Results and discussions

3.1. Synthesis and structure of catalysts

Compared to unsaturated oxime or imine functional group, the pyridine moiety is stable towards ligand hydrogenation.^{8a} Accordingly, the bipyridine or phenanthroline moiety has frequently been used as a desirable feature in developing efficient and robust catalysts.^{10g} Herein, we designed a phenanthroline-containing aminopyridine ligand DPA-Dmphen, which was readily accessible via a directly alkylation of bis(pyridin-2-ylmethyl)amine with an equivalent of 2-

(chloromethyl)-9-methyl-1,10-phenanthroline (Fig. S1, S2 and S3[†]). Complexation of DPA-Dmphen with Co(H₂O)₆(ClO₄)₂ and Ni(H₂O)₆(ClO₄)₂ in methanol proceeded smoothly at room temperature to afford the dicationic complexes of general formula [M(Dmphen-DPA)(H₂O)](ClO₄)₂, M=Co (**1**) and M=Ni (**2**). Then diethyl ether diffusion yielded the crystalline material of red **1** and pale brown **2**, respectively, which were confirmed by elemental analysis and ESI-MS spectra (Fig. S4 and S5[†]).

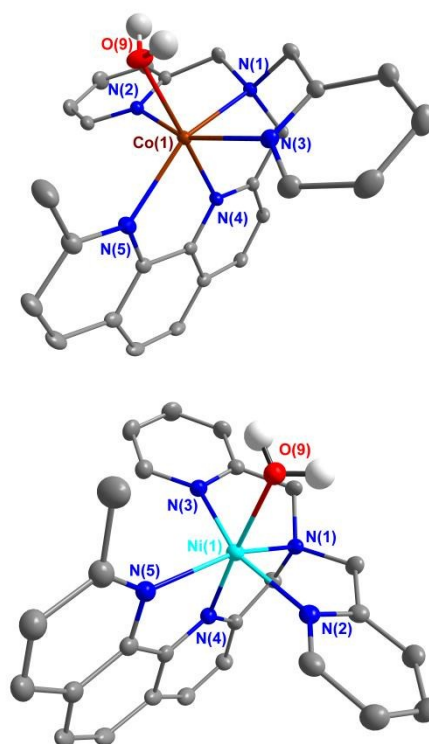


Fig. 2 Crystal structures of complexes **1** and **2** (the hydrogen atoms, solvent molecules and ClO₄²⁻ anions are omitted for clarity).

The crystal structures of complexes **1** and **2** are given in Fig. 2 with selected bond lengths and angles listed in Table S1, which were established by means of single crystal X-ray diffraction. For the isostructural complexes **1** and **2**, the metal centers Co(II) and Ni(II) reside in a distorted octahedral geometry. The Dmphen-DPA acts as the pentadentate ligand, leaving one coordination side of the transition metal available for water molecule. The M–N bond lengths fall in the range of the expected values where the M–N(5) bonds are significantly longer by about 0.2 Å than the M–N(4) bonds. The M–O bond lengths range from 2.0701(14) to 2.0683(19) Å, which are similar to those in the complexes [(bztphen)Co(H₂O)]²⁺ and [(PY5Me₂)Co(H₂O)]²⁺.^{10b, 12}

3.2. Photocatalytic hydrogen production

Based on the literature, cyclometalated iridium complexes, such as [Ir(ppy)₂(bpy)]PF₆, displayed considerably high efficiency for hydrogen evolution in combination with triethanolamine or triethylamine (TEA) as electron donor in some Fe- and Co-

based photocatalytic systems.¹⁷ Hence, the photocatalytic H₂ production activity of the complex **1** was first tested by using [Ir(ppy)₂(bpy)]PF₆ as photosensitizer and TEA as the electron donor. CH₃CN-H₂O (1/3, v/v) mixed solvent was chosen as the reaction medium, in which acetonitrile was used to achieve dissolution of the photosensitizer. Upon irradiation with a 300 W Xe lamp ($\lambda > 400$ nm), the amount of H₂ generated from the reaction system [Ir(ppy)₂(bpy)]PF₆/**1**/TEA was established by gas chromatography with a thermal conductivity detector. A series of factors such as pH value and the concentration of each component were studied to obtain the optimal photocatalysis condition (Fig.3a to 3c). As a result, an optimized H₂ evolution system containing 0.1 mM **1**, 0.5 mM [Ir(ppy)₂(bpy)](PF₆), and

10 vol% TEA in 5 mL CH₃CN-H₂O (1/3, v/v) at pH 10 was able to release a total amount of 105 μ mol H₂ (TON = 210) after 4 h of irradiation. Control experiments in the absence of one of the components (i.e., TEA, [Ir(ppy)₂(bpy)](PF₆), or **1**) resulted in little to no H₂ production, indicating that all three components are required for the evolution of H₂. Regarding the high cost of the photosensitizer [Ir(ppy)₂(bpy)]PF₆, the use of inexpensive and commonly available organic dyes, such as Erythrosin B (EB) and Fluorescein (Fl), instead of [Ir(ppy)₂(bpy)]PF₆ was studied in association with **1** under irradiation for 4 h and the same experimental conditions. As shown in Fig. 3d, the TON of H₂ produced by **1** was drastically decreased to 14 and 5 in the presence of Fl and EB, respectively.

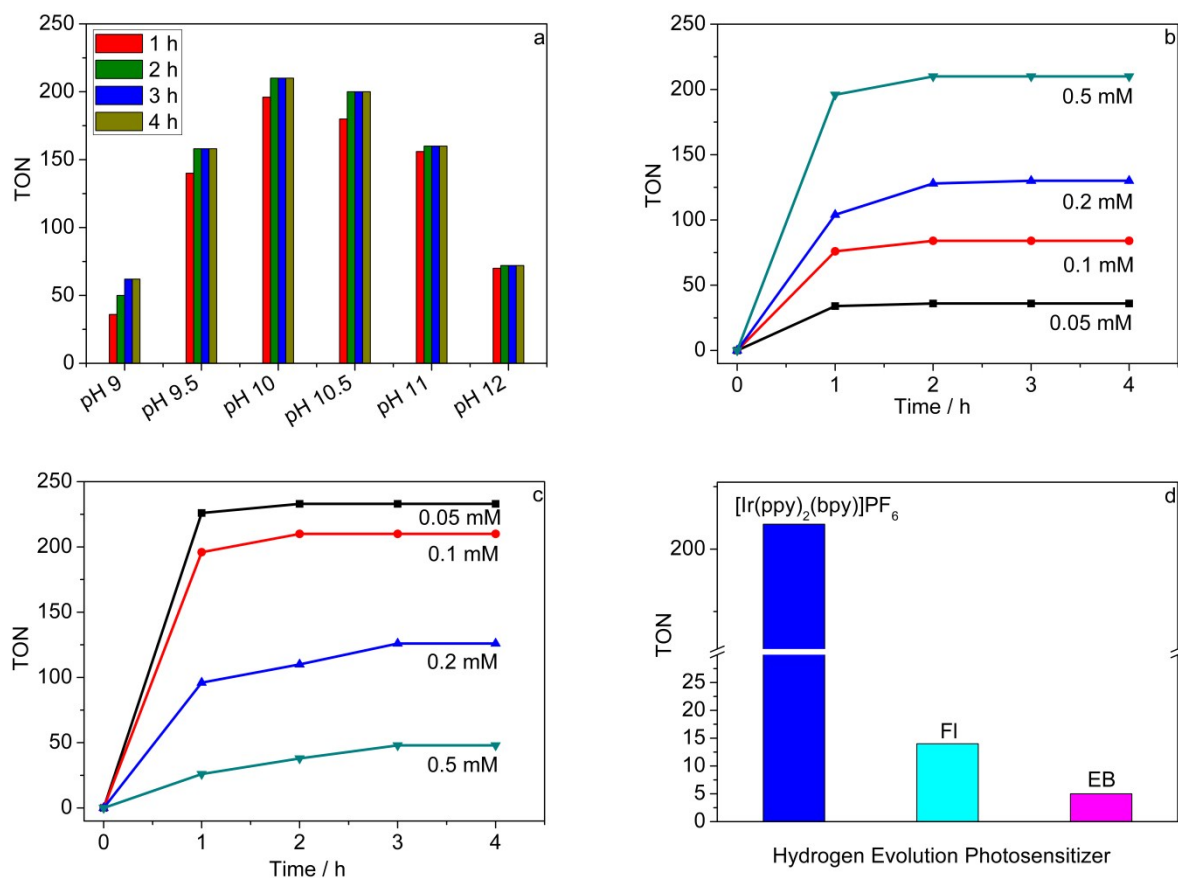


Fig. 3 (a) Photocatalytic H₂ evolution at different pH values in CH₃CN-H₂O(1/3, v/v) containing 10 vol% TEA, [Ir(ppy)₂(bpy)](PF₆) (0.5 mM) and complex **1**(0.1 mM); (b) the dependence of H₂ evolution on the concentration of [Ir(ppy)₂(bpy)](PF₆) from 0.05 mM to 0.5 mM; (c) H₂ evolution as a function of concentration of the complex **1** from 0.05 mM to 0.5 mM; (d) photocatalytic hydrogen production from CH₃CN-H₂O (1/3, v/v) solution (5 mL) at pH 10 containing a photosensitizer (0.5 mM), TEA (10 vol %), and the complex **1** (0.1 mM).

Likewise, the catalytic performance of analogous complex **2** was also optimized in the same way that used for the complex **1**. It was found that the trends of the reaction condition dependence on hydrogen evolution over the system [Ir(ppy)₂(bpy)]PF₆/**2**/TEA agreed closely with those over the system [Ir(ppy)₂(bpy)]PF₆/**1**/TEA (Fig. S6-S8[†]). In the aspect of reaction phenomenon, the color of the reaction system [Ir(ppy)₂(bpy)]PF₆/**2**/TEA changed from yellow to brown within 2 min after irradiating the solution with visible light,

which was also observed in the system [Ir(ppy)₂(bpy)]PF₆/**1**/TEA, but the complex **2** displayed much lower H₂ evolution activity than the complex **1**, with a maximum TON of 11 (Fig.4). For comparison, simple metal salts Co(H₂O)₆(ClO₄)₂ and Ni(H₂O)₆(ClO₄)₂ were also tested for the photocatalytic H₂ evolution in combination with [Ir(ppy)₂(bpy)](PF₆) under the optimized conditions. As shown in Fig.4, the results clearly indicated a certain activity of H₂ evolution, but less than that of corresponding metal complexes,

suggesting the H₂ production of complexes **1** and **2** is indeed derived from itself rather than the metal ions liberated.

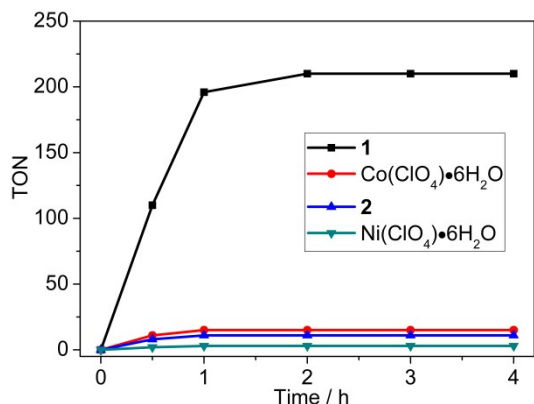


Fig. 4 Time dependence of hydrogen production using **1** (0.1 mM), **2** (0.1 mM), Co(H₂O)₆(ClO₄)₂ (0.1 mM) and Ni(H₂O)₆(ClO₄)₂ (0.1 mM) under the following conditions: [Ir(ppy)₂(bpy)](PF₆) (0.5 mM), 10 vol % TEA in CH₃CN-H₂O (1/3, v/v) solution (5 mL) at pH 10.

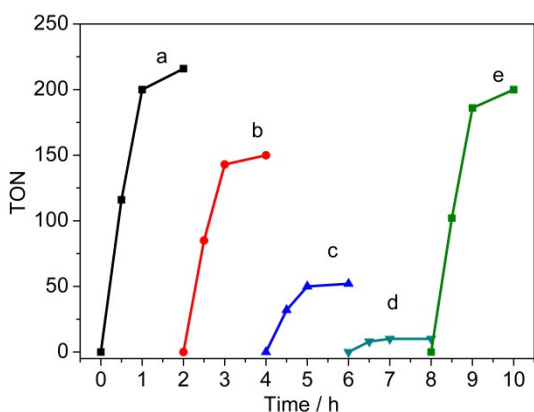


Fig. 5 Cycle runs (a-d) for the photocatalytic H₂ with readdition of [Ir(ppy)₂(bpy)]PF₆ (2.5 μmol) to the system every two hours; (e) simultaneous readdition of **1** (0.5 μmol) and [Ir(ppy)₂(bpy)]PF₆ (2.5 μmol) to the solution after 4 cycles.

After approximately 2 h of irradiation, the hydrogen-evolution leveled off due to the decomposition of at least one component of the [Ir(ppy)₂(bpy)]PF₆ and the complex **1** in the presence of a large excess of TEA. To identify the reason(s) for the cease of H₂ generation, extra [Ir(ppy)₂(bpy)]PF₆, **1** or TEA, was readded when the photocatalytic system failed to release H₂. The H₂ production could not be recovered when extra **1** (0.5 μmol) or TEA (10%, v/v) was added to the inactive system. However, as shown in Fig.5, the H₂ production was partially recovered, and the extra H₂ yield of 150 TON (vs. **1**) was recorded in the case of extra [Ir(ppy)₂(bpy)]PF₆ (2.5 μmol) to be added to the inactive system mentioned above. Furthermore, we found that the photocatalytic system was completely inactive after 4 cycle runs in spite of readdition of

[Ir(ppy)₂(bpy)]PF₆. In contrast, the durative H₂ production had been observed when the extra **1** (0.5 μmol) and [Ir(ppy)₂(bpy)]PF₆ (2.5 μmol) were simultaneously added to the completely inactive system, implying the photo-degradations of [Ir(ppy)₂(bpy)]PF₆ and **1** were the major reasons of the inactivation of photocatalytic system and [Ir(ppy)₂(bpy)]PF₆ decomposed faster than the complex **1** in the photolysis process.

3.3. Electrochemistry properties

The redox potential of the complexes is crucial to understand the electron transfer in photocatalytic process. Cyclic voltammetry studies were performed in acetonitrile with Bu₄NPF₆ as supporting electrolyte under nitrogen atmosphere. The electrochemical redox processes of complexes **1** and **2** are shown in Fig. 6, and the reduction potentials are versus Fc⁺/Fc and are summarized in Table S2. Each of the complexes exhibited multiple redox processes, and therefore this is consistent with the rich electrochemical behavior of Co- and Ni-based molecular catalysts.^{10e, 18} First, the ligand Dmphen-DPA displayed electrochemically silent in the experimental potential range, suggesting all redox processes for **1** and **2** could be assigned as metal-based events. The cyclic voltammogram of complex **1** showed a reversible reduction at $E_{1/2} = -1.43$ V assigned to Co(II)/Co(I), with a second irreversible reduction peak at -2.22 V. A quasi-reversible oxidative wave at -0.02 V could further be assigned to the Co(II)/Co(III) oxidation event. The nickel complex in **2** exhibited a reversible Ni(II)/Ni(I) reduction at -1.42 V. At more negative potential, two closely spaced reductions occurred at -2.08 and -2.21 V, which had not been further investigated but likely involve both, proton of water and metal based Ni(I)/Ni(0) reductions.

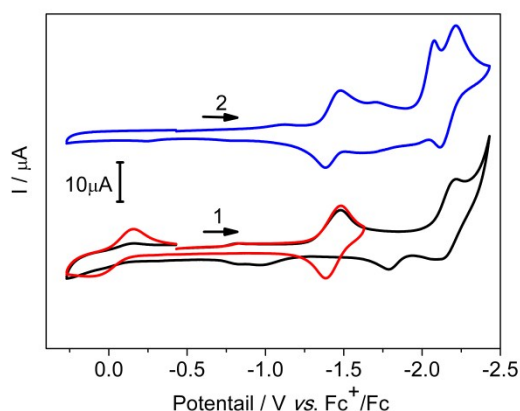


Fig. 6 Cyclic voltammograms of **1** (0.5 mM) and **2** (0.5 mM) measured in acetonitrile (0.1 M NBu₄PF₆, $v = 100$ mV s⁻¹).

To evaluate possible electrochemical activities for the reduction of protons, cyclic voltammograms of compounds **1** and **2** in CH₃CN were recorded in the presence of acetic acid (HOAc, $pK_a = 22.3$ in acetonitrile).¹⁹ For the complex **1**, on addition of two equivalents HOAc, the first peak of **1** at -1.43 V

increased only slightly and a new reduction wave appeared at -2.09 V, with the onset of current increase occurred at -1.70 V (Fig. 7a). Upon the addition of more acid, the peak at -1.43 V was essentially unaffected, whereas the current of the new wave was greatly enhanced and the onset potential of the new wave was positively shifted (Fig. 7a and S9[†]). For a convenient comparison, under the same conditions in CH_3CN with no complex **1**, HOAc at 5 mM concentration was reduced to H_2 at -2.3 V (Fig. 7a, dash line). It is evident that the electrochemical response of **1** to the addition of HOAc observed at -2.09 V is well within the acetonitrile solvent window.²⁰ This indicates that the complex **1** is the active species for electrocatalytic proton reduction.^{13, 21} Likewise, addition of HOAc to the solution of **2** resulted in a simultaneous broadening and increase in the current observed for the second reduction process. The height of the second reduction peak continuously grew with increased acid concentration (Fig. S9[†]), suggesting that **2** is also an efficient electrocatalyst for proton reduction.

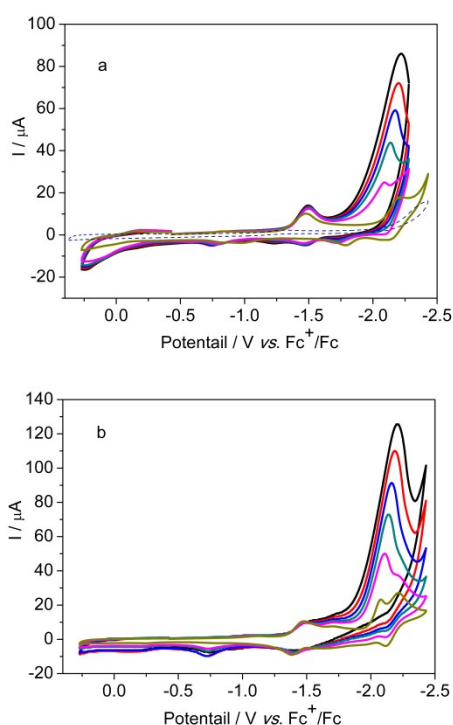


Fig. 7 Electrochemical response of 0.5 mM **1**(a) and **2** (b) to addition of acetic acid (0, 1, 2, 3, 4, 5 mM) in acetonitrile (0.1 M NBu₄PF₆, $\nu = 100$ mV s⁻¹). The dashed line represents the blank electrochemical scan for acetic acid (5 mM) in the absence of electrocatalyst.

In both cases addition of HOAc triggers a significant current enhancement at the potential that is more negative than the M(II)/M(I) reduction potential. In view of the $E^\circ(\text{HOAc}/\text{H}_2)$ value of -1.46 V in acetonitrile,¹⁹ the overpotentials for the electrocatalytic reduction of protons from HOAc were determined to be 0.48 V and 0.46 V for the complex **1** and **2**, respectively,^{1b} which are close to the overpotential value of about 0.40 V in similar experiments utilizing a cobalt catalyst $[(\text{CF}_3\text{PY5Me}_2)\text{Co}(\text{CH}_3\text{CN})](\text{CF}_3\text{SO}_3)_2$ and HOAc as proton

source.^{8a} To test the catalytic capacity of **1**, we obtained the $i_{\text{cat}}/i_{\text{p}}$ ratio versus the concentration of HOAc plots, where i_{cat} stands for catalytic current intensity in the presence of HOAc and i_{p} for the noncatalytic current intensity in the absence of HOAc. As shown in Fig. 8, the $i_{\text{cat}}/i_{\text{p}}$ ratio increased linearly when HOAc concentration was below 5 mM. At higher HOAc concentration (> 5 mM), the $i_{\text{cat}}/i_{\text{p}}$ ratio was independent of the acid concentration, and the resulting $i_{\text{cat}}/i_{\text{p}}$ value of **1** (≈ 12) was higher than those of Co- and Fe-based molecular catalysts such as $[\text{Co}(\text{PY5Me}_2)]^{2+}$, $(\mu\text{-pdt})[\text{Fe}(\text{CO})_2(\text{PTA}\cdot\text{H}^+)]_2$ and $(\mu\text{-pdt})[\text{Fe}_2(\text{CO})_5\text{Ph}_2\text{PCH}_2\text{Py}]$.^{20, 22} As expected, the complex **2** ($i_{\text{cat}}/i_{\text{p}} = 7$) exhibited a slightly lower catalytic capacity than **1**.

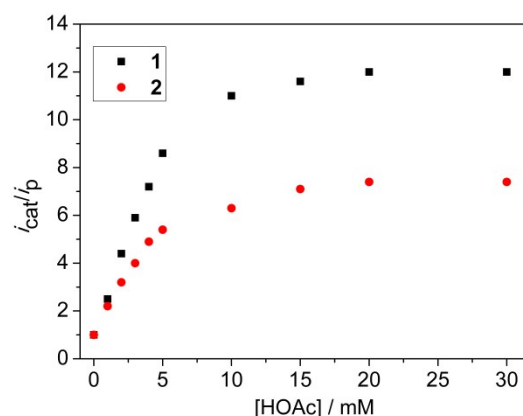


Fig. 8 Plots of the $i_{\text{cat}}/i_{\text{p}}$ ratio as a function of the concentration of HOAc for **1** (0.5 mM) and **2** (0.5 mM). $i_{\text{cat}}/i_{\text{p}}$ values were measured at the potential of pinnacle. The scan rate was 100 mV s⁻¹.

3.4. The discussion of photocatalytic H₂ production

Under photocatalytic conditions, two mechanisms may be proposed for the electron transfer pathways: a reductive quenching process or an oxidative quenching process.^{17d} To discriminate the charge transfer pathways in photocatalysis process, the steady-state photoluminescence properties of the systems $[\text{Ir}(\text{ppy})_2(\text{bpy})]\text{PF}_6/\mathbf{1}/\text{TEA}$ and $[\text{Ir}(\text{ppy})_2(\text{bpy})]\text{PF}_6/\mathbf{2}/\text{TEA}$ were investigated in acetonitrile aqueous solution (Fig. 9). Consistent with the previous photoluminescence studies,¹⁴ the $[\text{Ir}(\text{ppy})_2(\text{bpy})]\text{PF}_6$ sample in $\text{CH}_3\text{CN}-\text{H}_2\text{O}$ (1/3, v/v) solution exhibited a strong emission peak at about 500 nm to 700 nm. No significant decreases in fluorescence intensity were observed upon addition of either **1** or **2**. However, when TEA was introduced, the intensity of this emission band immediately showed a decrease, indicating the excited state of the iridium photosensitizer should be reductively quenched by TEA rather than oxidative quenching by **1** and **2**.

The reductive quenching of the excited state of $[\text{Ir}(\text{ppy})_2(\text{bpy})](\text{PF}_6)$ could give a reduced species $[\text{Ir}(\text{ppy})_2(\text{bpy})]^0$ ($E^\circ = -1.81$ V vs. Fc^+/Fc for $[\text{Ir}(\text{ppy})_2(\text{bpy})]^+ / [\text{Ir}(\text{ppy})_2(\text{bpy})]$),^{17c} which is capable of reducing the complex **1** to Co^{I} species. Protonation of the low-valent cobalt center then generates a $[\text{H}-\text{Co}^{\text{III}}]^{2+}$ intermediate.^{5b}

Under basic conditions, H₂ production requires further reduction of this intermediate to generate a [H-Co^{II}]⁺ active species.^{8a, 13} Because of the more negative reduction potential of the intermediate [H-Co^{III}]²⁺ (onset reduction potential at -1.70 V vs. Fc⁺/Fc), the photosensitizer should possess a higher reduction potential to achieve the electron transfer. Accordingly, the [Ir(ppy)₂(bpy)]PF₆ displayed the highest activity relative to organic dyes.

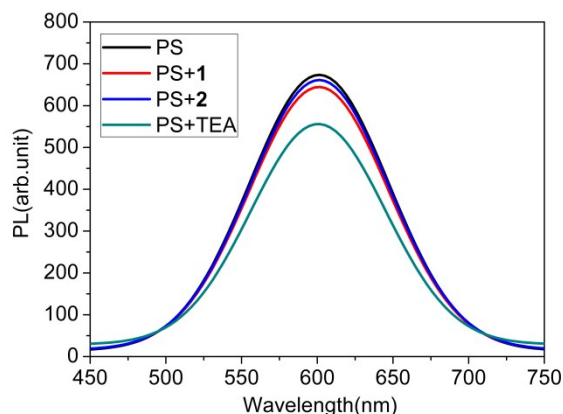


Fig. 9 The emission spectra of [Ir(ppy)₂(bpy)]PF₆ (0.1 mM) in CH₃CN-H₂O (1/3, v/v) solution in the presence of **1** (0.1 mM), **2** (0.1 mM) or 10 vol% TEA (pH 10) acetonitrile aqueous solution.

Both complexes (*i.e.*, **1** and **2**) were active for electrocatalytic proton reduction from weak acid in acetonitrile, while the cobalt complex **1** was much more active than the nickel complex **2** under photocatalytic conditions. Besides **2**, the nickel complexes of pentadentate ligand such as [NiBr(aPPy)]Br, [Ni(bpy₂PYMe)(CH₃CN)](BF₄)₂ and [Ni(CF₃SO₃)(Py₂^{Ts}tacn)](CF₃SO₃) generally showed a low photocatalytic activity in previous reports.^{8, 13} Recent experimental and theoretical studies by Lloret-Fillol and colleagues indicated the more acidic character of [Ni^{III}-H] species, which renders the protonation of Ni^I intermediates more difficult in basic pH conditions.¹³ This could provide a rationale for the low photocatalytic ability of **2** compared to **1**. Therefore, further studies are aimed at improving the H₂-evolving activity of **2** with other photosensitizers under certain conditions (for instance at acidic pH).

4. Conclusions

We have presented a new aminopyridine ligand [(9-methyl-1,10-phenanthroline-2-yl)methyl]bis-(pyridin-2-ylmethyl)amine and its corresponding metal complexes of Co²⁺ (**1**) and Ni²⁺ (**2**). Both complexes were well-behaved electrochemically and showed a catalytic current for proton reduction from acetic acid with overpotentials for **1** (0.48 V vs. Fc⁺/Fc) and **2** (0.46 V vs. Fc⁺/Fc). In the presence of a photosensitizer [Ir(ppy)₂(bpy)](PF₆) and an electron donor TEA, the complex **1** evolved hydrogen when exposed to visible-light light, with a highest TON of 210 under optimal conditions. In contrast, the complex **2** displayed

much lower photocatalytic H₂ production activity than complex **1** under the same conditions.

Acknowledgements

The authors thank the National Natural Science Foundation China (grant numbers 21101153, 21231003 and 21203195) for financial support.

Notes and references

^a State Key Laboratory of Structural Chemistry, Fujian Institute of Research on the Structure of Matter, Chinese Academy of Sciences, Fuzhou, Fujian 350002, P. R. China; E-mail: ccn@fjirsm.ac.cn

^b University of Chinese Academy of Sciences, Beijing, 100049, China

† Electronic Supplementary Information (ESI) available: [Fig. S1 - Fig. S9, Table S1 and Table S2]. See DOI: 10.1039/b000000x/

- (a) F. Wang, W. G. Wang, H. Y. Wang, G. Si, C. H. Tung and L. Z. Wu, *ACS Catal.*, 2012, **2**, 407; (b) M. Wang, L. Chen and L. Sun, *Energy Environ. Sci.*, 2012, **5**, 6763; (c) V. Artero and M. Fontecave, *Chem. Soc. Rev.*, 2013, **42**, 2338.
- (a) N. S. Lewis and D. G. Nocera, *Proc. Natl. Acad. Sci. USA*, 2006, **103**, 15729; (b) L. Sun, B. Åkermark and S. Ott, *Coord. Chem. Rev.*, 2005, **249**, 1653; (c) A. Kudo, *Int. J. Hydrogen. Energ.*, 2007, **32**, 2673.
- (a) M. Wang, Y. Na, M. Gorlov and L. Sun, *Dalton Trans.*, 2009, 6458; (b) X. Chen, S. Shen, L. Guo and S. S. Mao, *Chem. Rev.*, 2010, **110**, 6503; (c) J. Ran, J. Zhang, J. Yu, M. Jaroniec and S. Z. Qiao, *Chem. Soc. Rev.*, 2014, **43**, 7787.
- (a) H. Y. Wang, W. G. Wang, G. Si, F. Wang, C. H. Tung and L. Z. Wu, *Langmuir*, 2010, **26**, 9766; (b) X. Li, M. Wang, D. Zheng, K. Han, J. Dong and L. Sun, *Energy Environ. Sci.*, 2012, **5**, 8220; (c) T. Yu, Y. Zeng, J. Chen, Y. Y. Li, G. Yang and Y. Li, *Angew. Chem. Int. Ed.*, 2013, **52**, 5631.
- (a) P. Du, K. Knowles and R. Eisenberg, *J. Am. Chem. Soc.*, 2008, **130**, 12576; (b) V. Artero, M. Chavarot-Kerlidou and M. Fontecave, *Angew. Chem. Int. Ed.*, 2011, **50**, 7238; (c) W. R. McNamara, Z. Han, P. J. Alperin, W. W. Brennessel, P. L. Holland and R. Eisenberg, *J. Am. Chem. Soc.*, 2011, **133**, 15368; (d) K. Kawano, K. Yamauchi and K. Sakai, *Chem. Commun.*, 2014, **50**, 9872.
- (a) M. P. McLaughlin, T. M. McCormick, R. Eisenberg and P. L. Holland, *Chem. Commun.*, 2011, **47**, 7989; (b) W. Zhang, J. Hong, J. Zheng, Z. Huang, J. Zhou and R. Xu, *J. Am. Chem. Soc.*, 2011, **133**, 20680; (c) Z. Han, W. R. McNamara, M. S. Eum, P. L. Holland and R. Eisenberg, *Angew. Chem. Int. Ed.*, 2012, **51**, 1667; (d) Z. Han, F. Qiu, R. Eisenberg, P. L. Holland and T. D. Krauss, *Science*, 2012, **338**, 1321; (e) M. A. Gross, A. Reynal, J. R. Durrant and E. Reisner, *J. Am. Chem. Soc.*, 2013, **136**, 356; (f) H. N. Kagalwala, E. Gottlieb, G. Li, T. Li, R. Jin and S. Bernhard, *Inorg. Chem.*, 2013, **52**, 9094; (g) L. Yin, Y. P. Yuan, S. W. Cao, Z. Zhang and C. Xue, *RSC Advances*, 2014, **4**, 6127; (h) O. R. Luca, S. J. Konezny, J. D. Blakemore, D. M. Colosi, S. Saha, G. W. Brudvig, V. S. Batista and R. H. Crabtree, *New J. Chem.*, 2012, **36**, 1149.
- (a) Y. Hou, B. L. Abrams, P. C. K. Vesborg, M. E. Björketun, K. Herbst, L. Bech, A. M. Setti, C. D. Damsgaard, T. Pedersen, O. Hansen, J. Rossmeisl, S. Dahl, J. K. Nørskov and I. Chorkendorff,

- Nat Mater*, 2011, **10**, 434; (b) H. I. Karunadasa, E. Montalvo, Y. Sun, M. Majda, J. R. Long and C. J. Chang, *Science*, 2012, **335**, 698.
8. (a) M. Nippe, R. S. Khnayzer, J. A. Panetier, D. Z. Zee, B. S. Olaiya, M. Head-Gordon, C. J. Chang, F. N. Castellano and J. R. Long, *Chem. Sci.*, 2013, **4**, 3934; (b) C. Bachmann, M. Guttentag, B. Spingler and R. Alberto, *Inorg. Chem.*, 2013, **52**, 6055.
9. (a) C. V. Krishnan and N. Sutin, *J. Am. Chem. Soc.*, 1981, **103**, 2141; (b) C. V. Krishnan, B. S. Brunshwig, C. Creutz and N. Sutin, *J. Am. Chem. Soc.*, 1985, **107**, 2005; (c) H. A. Schwarz, C. Creutz and N. Sutin, *Inorg. Chem.*, 1985, **24**, 433.
10. (a) J. P. Bigi, T. E. Hanna, W. H. Harman, A. Chang and C. J. Chang, *Chem. Commun.*, 2010, **46**, 958; (b) Y. Sun, J. P. Bigi, N. A. Piro, M. L. Tang, J. R. Long and C. J. Chang, *J. Am. Chem. Soc.*, 2011, **133**, 9212; (c) W. M. Singh, T. Baine, S. Kudo, S. Tian, X. A. N. Ma, H. Zhou, N. J. DeYonker, T. C. Pham, J. C. Bollinger, D. L. Baker, B. Yan, C. E. Webster and X. Zhao, *Angew. Chem. Int. Ed.*, 2012, **51**, 5941; (d) S. Varma, C. E. Castillo, T. Stoll, J. Fortage, A. G. Blackman, F. Molton, A. Deronzier and M. N. Collomb, *Phys Chem Chem Phys*, 2013, **15**, 17544; (e) Y. Sun, J. Sun, J. R. Long, P. Yang and C. J. Chang, *Chem. Sci.*, 2013, **4**, 118; (f) R. S. Khnayzer, V. S. Thoi, M. Nippe, A. E. King, J. W. Jurss, K. A. El Roz, J. R. Long, C. J. Chang and F. N. Castellano, *Energy Environ. Sci.*, 2014, **7**, 1477; (g) L. Tong, R. Zong and R. P. Thummel, *J. Am. Chem. Soc.*, 2014, **136**, 4881.
11. B. Shan, T. Baine, X. A. N. Ma, X. Zhao and R. H. Schmechl, *Inorg. Chem.*, 2013, **52**, 4853.
12. P. Zhang, M. Wang, F. Gloaguen, L. Chen, F. Quentel and L. Sun, *Chem. Commun.*, 2013, **49**, 9455.
13. A. Call, Z. Codolà, F. Acuña-Parés and J. Lloret-Fillol, *Chem. Eur. J.*, 2014, **20**, 6171.
14. M. S. Lowry, W. R. Hudson, R. A. Pascal and S. Bernhard, *J. Am. Chem. Soc.*, 2004, **126**, 14129.
15. G. R. Newkome, K. J. Theriot, V. K. Gupta, F. R. Fronczek and G. R. Baker, *J. Org. Chem.*, 1989, **54**, 1766.
16. A. Thapper, A. Behrens, J. Fryxelius, M. H. Johansson, F. Prestopino, M. Czaun, D. Rehder and E. Nordlander, *Dalton Trans.*, 2005, 3566.
17. (a) J. I. Goldsmith, W. R. Hudson, M. S. Lowry, T. H. Anderson and S. Bernhard, *J. Am. Chem. Soc.*, 2005, **127**, 7502; (b) Y. J. Yuan, Z. T. Yu, H. L. Gao, Z. G. Zou, C. Zheng and W. Huang, *Chem. Eur. J.*, 2013, **19**, 6340; (c) P. Zhang, M. Wang, Y. Na, X. Li, Y. Jiang and L. Sun, *Dalton Trans.*, 2010, **39**, 1204; (d) P. Zhang, P. A. Jacques, M. Chavarot-Kerlidou, M. Wang, L. Sun, M. Fontecave and V. Artero, *Inorg. Chem.*, 2012, **51**, 2115.
18. S. Losse, J. G. Vos and S. Rau, *Coord. Chem. Rev.*, 2010, **254**, 2492.
19. G. A. N. Felton, R. S. Glass, D. L. Lichtenberger and D. H. Evans, *Inorg. Chem.*, 2006, **45**, 9181.
20. R. Mejia-Rodriguez, D. Chong, J. H. Reibenspies, M. P. Soriaga and M. Y. Darensbourg, *J. Am. Chem. Soc.*, 2004, **126**, 12004.
21. S. Jiang, J. Liu, Y. Shi, Z. Wang, B. Akermark and L. Sun, *Polyhedron*, 2007, **26**, 1499.
22. (a) A. E. King, Y. Surendranath, N. A. Piro, J. P. Bigi, J. R. Long and C. J. Chang, *Chem. Sci.*, 2013, **4**, 1578; (b) D. Chong, I. P. Georgakaki, R. Mejia-Rodriguez, J. Sanabria-Chinchilla, M. P. Soriaga and M. Y. Darensbourg, *Dalton Trans.*, 2003, 4158; (c) P. Li, M. Wang, L. Chen, J. Liu, Z. Zhao and L. Sun, *Dalton Trans.*, 2009, 1919.